IOP PUBLISHING JOURNAL OF PHYSICS D: APPLIED PHYSICS

J. Phys. D: Appl. Phys. **43** (2010) 425301 (6pp) doi:10.1088/0022-3727/43/42/425301

Nitrogen incorporation into GaAs lattice as a result of the surface cavitation effect

R K Savkina and A B Smirnov

V. Lashkaryov Institute of Semiconductor Physics at NAS of Ukraine, pr. Nauki 41, 03028 Kiev, Ukraine

E-mail: r_savkina@lycos.com

Received 21 April 2010, in final form 21 August 2010
Published 5 October 2010
Online at stacks.iop.org/JPhysD/43/425301

Abstract

Semi-insulating gallium arsenide was exposed to cavitation impact initiated by focusing a high-frequency acoustic wave into liquid nitrogen. Optical and atomic force microscopy methods were used for the analysis of surface morphology. Formation of microstructures as well as change in the chemical composition of the surface are observed. The morphology of the structures is highly dependent on the acoustic parameters. Raman spectroscopy data have confirmed the incorporation of nitrogen atoms into the GaAs lattice and Ga–N bond formation in the region of maximal structural change due to the cavitation impact.

(Some figures in this article are in colour only in the electronic version)

1. Introduction

Nowadays, ultrasound (US) technology is widely applied in mechanical engineering, cleaning industries and health diagnosis [1–3]. In addition, US has proven to be a useful technique for generating novel materials [4–8].

The chemical effect of US arises from acoustic cavitation, which is the fundamental process of the formation and collapse of bubbles in a liquid exposed to intense sound. Considerable local heating and high pressure accompany this process. The bubble temperature reaches thousands of kelvins during collapse, pressure equals several hundred megapascals, and heating and cooling rates are above $10^{10}\,\mathrm{K\,s^{-1}}$ [4]. It should also be noted that plasma generation is possible in a cavitating liquid [9]. These extreme conditions are exploited for preparing amorphous metals, carbides, oxides and sulfides from dissolved solution precursors. It should seem that using cavitation phenomenon for solid surface modification is an attractive approach. However, it is difficult to control cavitation. This is in particular related to cavitation at surfaces. The destructive action of heterogeneous bubble nucleation at surfaces is a grave disadvantage in many industrial systems.

Controlled multibubble surface cavitation can be achieved using a hydrophobic surface patterned with microcavities [10]. In addition, it is considered that megacycle US produces controlled acoustic cavitation and does not cause damage of surfaces [2]. In this work, we demonstrate our effort to control surface cavitation by manipulation of the acoustic parameters. We describe experimental results on modification that occurs on the gallium arsenide surface subjected to megasonic cavitation exposure controlled by manipulation of the acoustic frequency. Most of the experimental works concerning acoustic cavitation have been carried out in water and a few organic liquids near room temperature. We initiate cavitation in liquid nitrogen (LN_2). Our intention was to initiate a reaction between nitrogen and gallium arsenide substrate with the aim of synthesizing $GaAs_{1-x}N_x$ compound, which is of considerable current interest for applications in electronic and optoelectronic devices.

2. Experiment

Materials used in this study were undoped, semi-insulating ($\rho > 10^7\,\Omega\,\mathrm{cm}$), (0 0 1)-oriented gallium arsenide wafers of diameter about 40 mm and $420 \pm 10\,\mu\mathrm{m}$ thickness grown by the liquid-encapsulated Czochralski method. The samples were cut into 5 mm × 5 mm squares and were cleaned for 10 min in ethanol and then in distilled water. The initial surface roughness of the samples was found to be below 1 nm. The roughness is determined by the atomic force microscopy (AFM) method on a few randomly chosen areas of $2 \times 2\,\mu\mathrm{m}^2$. Metal strips (Cu–Ni alloy and manganine) were deposited on the sample edges. Their role will be discussed later.

The semiconductor surface was investigated using optical microscopy (NV2E, Carl Zeiss Jena), atomic force microscopy (Digital Instruments NanoScope IIIa AFM operating in the tapping mode) and Raman spectroscopy.

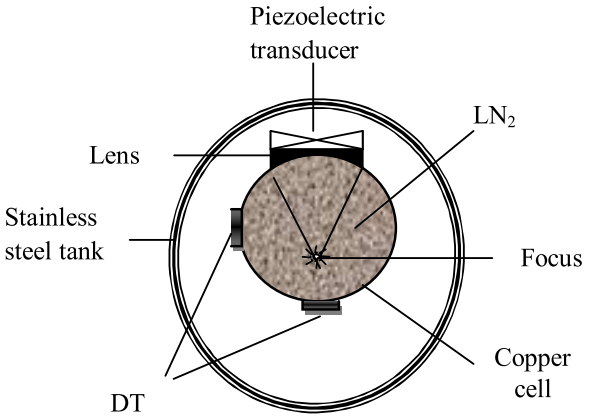

Figure 1. Experimental apparatus (top view); DT—diamond thermometers.

For cavitation activation, we used a high-frequency system (megahertz) with a focused energy resonator. It is known that the cavitation phenomenon occurs when acoustic intensity exceeds a certain threshold value. Utilization of focusing in our experiment has allowed increasing the power of the high-frequency acoustic system as well as concentrating exposure on the exact position of the solid surface so as not to affect the surrounding regions. It should also be noted that the operating temperature of LN_2 (78 K) is near the critical temperature of this fluid, and thermodynamic effect of cavitation can be easily attained.

The experimental setup consisted of a reactor vessel and US equipment. A pumped stainless steel tank with an internal copper cell filled with technical nitrogen was used for the reactor vessel (see figure 1). A ceramic piezoelectric transducer (PZT-19) with a diameter of 12 mm and a resonant frequency of 3 MHz (or 6 MHz) acoustically drove the cell. The output voltage of the US generator did not exceed 5 V, and the initial value of acoustic intensity W_{US} did not exceed 1 W cm^{-2}.

A cylindrical copper concentrator (lens) was used for US intensity enhancement. The intensity gain of the acoustic system (PZT + copper lens) was about 58. The acoustic matching of the PZT to copper lens is sufficient for satisfying the condition of transparent boundary (∼98%). The acoustic impedance in liquid nitrogen (of the order of 0.7×10^6 m^{-2} s^{-1}) is small as compared with the impedance of the copper lens (of the order of 3×10^7 m^{-2} s^{-1}). As a consequence, the ratio of the emitted acoustic power to the dissipated power is ∼55%.

The semiconductor target was placed inside the acoustically driven copper cell in the focus region (see figure 1). The maximal value of pressure was about ∼8 bar in the focus of the acoustic system.

3. Results and discussion

3.1. Surface characterization using optical and atomic force microscopy

We observed that the exposure of the semiconductor substrate to megasonic cavitation in LN_2 leads to the formation of micrometre-scale complex structures on the surface. Figure 2 shows the optical micrographs of the samples irradiated at varying acoustic parameters. After treatment of the GaAs sample at 3 MHz for 50 min in the acoustically driven copper cell, a ripple-like pattern and small rounded bumps with micrometre size develop (figure 2(*a*)). Small rings about 5–10 μm in diameter located in a random way are formed as well. The mean structure height was estimated from the AFM data to be 300–500 nm as the modified region integrally is below the original surface.

The reduction of acoustic intensity at the same frequency decreases the effective size of the zone of liquid undergoing cavitation and thereby results in a decrease in the impact region. The character of surface modification is more random with continuity violation. Small pits are also visible on the surface.

The increase in the processing frequency to 6 MHz results in the formation of separated circular regions with submicrometre structures inside (figure 2(*b*)). Figure 3(*a*) shows the AFM image of a part of such a region, and its profile is depicted in the inset of figure 3(*c*). AFM studies revealed the presence of a rim around the structured region. Interior of the circular region is below the original surface. Figure 3(*b*) shows the submicrometre structures inside the circular region far from the rim. The roughness values of the above-mentioned surface regions are described by a surface height histogram (see figures 3(*c*) and (*d*), respectively). In these histograms, several local maxima marked by arrows are seen. One can separate four groups of structures with typical heights $h_i \sim 4.5$ nm, 25 nm, 50 nm and 75 nm. The average lateral size of the structures is of the order of 200–250 nm.

Thus, an array of microstructures was formed on the surface of gallium arsenide by processing it in a cavitating cryogenic liquid. It was found that a decrease in the characteristic dimension of structures on the semiconductor surface from micrometre to submicrometre size at a frequency changing from 3 to 6 MHz occurs and can be explained by the decrease in the mean bubble size.

3.2. Cavitation near solid surface

On the basis of various theoretical studies and experimental data on cavitation–surface interaction, it is possible to assert that microjet impact is the general physical mechanism responsible for the effect of cavitation near a solid surface [4]. The potential energy of an expanded bubble is converted into kinetic energy of a liquid jet that transfers it to the substrate atoms at the site of impact. Here, surface patterns are generated by 'initial' bubbles, formed in the liquid, and by 'secondary' bubbles, which are formed at the site of initial jet impacts. They represent shallow cavities and circular patterns, respectively [11].

Since we deal with multibubble cavitation in an acoustic field, the interaction between bubbles with the formation of compact groups, which are termed as small or large clusters, is possible. A distinguishing characteristic of large clusters is that they are observed in the field of standing wave, and they can be attracted by the surface and frequently appear like attached hemispheres under the influence of surface tension [12].

Apparently, the surface relief depicted in figure 2(*a*) is generated as a result of microjet impacts during collapses of

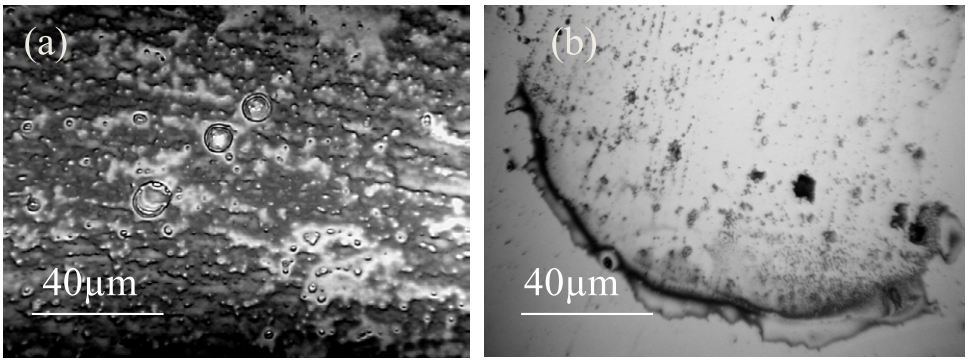

Figure 2. Optical micrographs of GaAs sample exposed to the acoustic cavitation in liquid nitrogen at 3 MHz for 50 min (*a*) and at 6 MHz for 15 min (*b*).

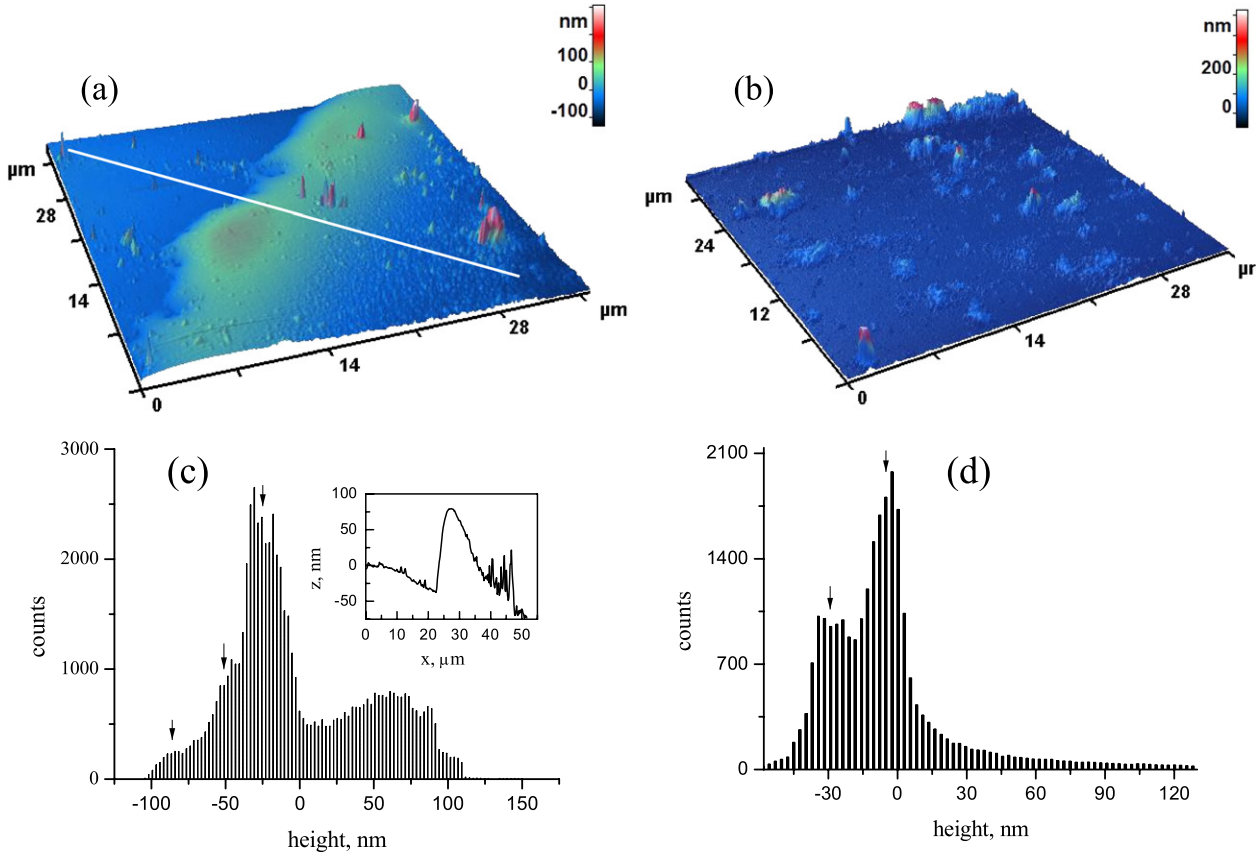

Figure 3. AFM image of the GaAs surface exposed to the acoustic cavitation in liquid nitrogen at 6 MHz: (*a*) part of the circular region framed in figure 2(*b*), (*b*) submicrometre structures inside the circular region, (*c*), (*d*) the histograms of a distribution of submicrometre structures over its height. Inset: cross-sectional view of the marked surface in (*a*).

both 'initial' and 'secondary' bubbles. At the same time, the surface relief shown in figure 2(*b*) is a demonstration of the collective bubbles' behaviour. It is quite possible that the minor increase in frequency from 3 to 6 MHz results in satisfying the condition of standing wave with the formation of large bubble clusters in the experimental cell. According to traces on the surface (figure 2(*b*)), we deal with large clusters with maximum radius up to the millimetre range.

It is well known that jets can reach velocities of hundreds of metres per second and can deposit enormous energy densities at the site of impact [4]. It is also known that GaAs is very susceptible to mechanical damage. In the case of GaAs, the brittle-to-ductile transition is estimated to be above 400 °C, below which the material is extremely brittle [13], although it was noted that GaAs is ductile under high pressures at a temperature lower than room temperature [14]. For example, the SEM image of a scratch made in the GaAs wafers at LN_2temperature clearly reveals ductile deformation behaviour in contrast to purely brittle fracture in a scratch made at room temperature [15].

Brittle materials deformed by cracking under collapsing bubbles' exposure [16]. However, we have not observed cracking after treatment, i.e. it can be assumed that the change

from brittle to ductile behaviour of GaAs target during contact loading at LN_2 temperature has occurred.

3.3. Surface characterization using electron probe microanalysis

It was found that various gaseous atoms (including nitrogen) can be strongly implanted into metal powders under ultrasonic cavitation [17]. In our experiment, one can expect that significant material intermixing at the impact sites takes place, and there is a probability for nitrogen atoms to incorporate into the GaAs target in the modified region.

The atomic composition of the microstructured gallium arsenide surfaces was investigated by means of energy dispersive x-ray spectroscopy (EDS). The chemical composition of the samples was studied on numerous randomly chosen areas of $5 \times 5\ \mu m^2$ between metal strips.

We found an inhomogeneous character of the incorporation of nitrogen atoms into the substrate lattice (from 5% to 7.5%) with simultaneous violation of the stoichiometric composition of GaAs after cavitation exposure. EDS analysis also indicated a high oxygen and carbon concentration for nitrided areas. At the same time, for some regions far from the metal strips the nitrogen atoms were not revealed while minor peaks corresponding to the elements P, S, K, Cl and Ca were identified. At this point we do not know the exact origin of the elements observed by the EDS technique, but we guess that they could have been dislodged from the walls of the experimental cell as well as from the technical nitrogen directly.

3.4. Raman scattering spectroscopy of microstructured GaAs

The properties of the microstructured GaAs samples were investigated using a macroscale Raman spectroscopy technique. Raman examination of the initial and irradiated surfaces of the samples under study was made in backscattering geometry using 514.5 nm line of an Ar^+ laser. The spectral resolution was $2\ cm^{-1}$. The Raman spectra were taken with a double grating spectrometer at room temperature. The signal was registered with a cooled phototube working in the photon counting mode.

The initial spectrum exhibits a one-mode character, i.e. longitudinal optic mode of the first order (LO1) at $292\ cm^{-1}$ (figure 4(*a*), curve 1). The Raman spectrum of the modified sample (during 50 min) has a complex structure and confirms the incorporation of nitrogen atoms into the GaAs lattice. In the range 200–300 cm^{-1}, we observe an increase in intensity and the red shift of the LO1 phonon band frequency to $281\ cm^{-1}$ (figure 4(*a*), curve 2), which can be connected with the effects of lattice strain and alloying [18]. In addition, transverse-optic (TO1) mode, which is forbidden for zinc-blende structure in backscattering geometry, develops in the Raman spectra at $267\ cm^{-1}$. On the low-wave-number side of TO1, a weak shoulder near $255\ cm^{-1}$, discussed by Mintairov *et al* as a strongly confined GaAs-like phonons LO_c [19], is identified. Such confinement (according to [19]) can be accomplished only by the N atoms. We also observe an additional line (LO_f) a few cm^{-1} below the LO1 phonon. The peak positions were

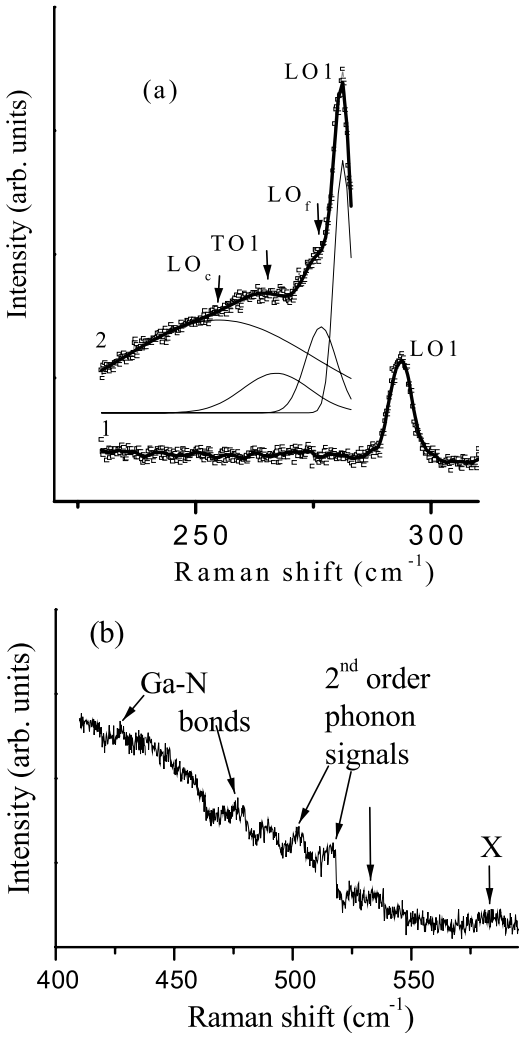

Figure 4. Room temperature Raman spectrum of a GaAs sample subjected to the acoustic cavitation effect in liquid nitrogen at 3 MHz: (*a*) in the frequency range $<300\ cm^{-1}$, initial spectrum (curve 1) and after processing (curve 2); (*b*) in the frequency range $>300\ cm^{-1}$ after processing. The dots in the figure are experimental data and the solid lines are fitting curves obtained by the Lorentzian model.

obtained from the corresponding Lorentz curves fitted to the experimental ones.

A close inspection of the Raman spectrum in the frequency range $>300\ cm^{-1}$ (figure 4(*b*)) detects the appearance of Ga–N local vibrational mode at about $475\ cm^{-1}$ [18, 19] and a weak peak near $426\ cm^{-1}$, which can be attributed also to the vibrations associated with Ga–N bonds [20]. The Raman features at frequencies above $490\ cm^{-1}$ are caused by second-order scattering by GaAs-like optical phonons, and they are labelled accordingly (figure 4(*b*)).

In our opinion, the violation of the selection rules as well as the shift of the GaAs-like modes and the appearance of additional modes in the Raman spectrum of the modified sample are possible due to the formation of $GaAs_{1-x}N_x$ alloy with a complex microstructure that depends on the nitrogen concentration and the character of nitrogen incorporation into the GaAs lattice.

It is well known that there exists a correlation between the location of LO1 mode and the value of x for $GaAs_{1-x}N_x$. In our case, however, it is difficult to determine the nitrogen concentration for $\omega_{LO1} = 281\,cm^{-1}$ unambiguously. In conformity with the data of [19] the location of LO1 band corresponds to $x > 5\%$. According to the results of EDS analysis, the nitrogen concentration is determined to be $x = 5$–7.5%. Thus, its value exceeds the N-solubility limit ($x = 2\%$), and nitrogen ordering has to take place [19].

From the Raman measurement of $GaAs_{1-x}N_x$ ($x \leqslant 5\%$) layers and the bond polarizability model analysis, it was deduced that ordering of the N and As atoms into trigonal $(GaN)_m(GaAs)_n$, $n = m = 1$, superlattice clusters in the lattice of $GaAs_{1-x}N_x$ alloy occurred [19]. The strain induced by the ordered $GaAs_{1-x}N_x$ microclusters results in the trigonal deformation of the surrounding GaAs bonds and changes the selection rules for the LO1 and TO1 phonons of the GaAs matrix. This is in good agreement with the appearance of the TO1 mode in our case. Moreover, the observation of the LO_c band and an additional line (LO_f) a few cm^{-1} below the LO1 phonon, which has been assigned to a folded LO phonon [21], may be taken as evidence of the local ordering of N atoms in the alloy lattice.

It has recently been shown [20] that $GaAs_{1-x}N_x$ with x above the N-solubility limit provides a two-mode Ga–N Raman signal which discriminates between Ga–N bonds isolated in the GaAs-like matrix and Ga–N vibrations in the N-rich hard boundary clusters. The corresponding modes emerge at 475 and 425 cm^{-1} and correlate with our observation.

Finally, concerning carbon and oxygen uncovered by the EDS technique, we could also expect their incorporation into the GaAs lattice. The additional peak at 583 cm^{-1} (figure 4(*b*), line X) can be explained by the local vibrational mode produced by C on the As site [22]. At the same time, we could not identify the occurrence of GaAs oxides by Raman analysis unambiguously. Additional experiments are, clearly, necessary.

Thus, Raman spectroscopy data have confirmed the incorporation of nitrogen atoms into the GaAs lattice with the formation of Ga–N bonds and local ordering of N atoms in the alloy lattice. In other words, the intracavity conditions during collapse are sufficient to result in the dissociation of N_2. We cannot prove that this process occurs thermally. However, the effects described above were obtained exclusively for samples with deposited Cu–Ni strips. Therefore, we suppose that the mechanism of catalytic dissociation of nitrogen on metal surface [23] in combination with extreme conditions of bubble collapse is verisimilar in our case. The dissociation barrier [24] of N_2 in the case of Ni is 92 kJ $mole^{-1}$ and in the case of Cu is 146 kJ $mole^{-1}$, i.e. much lower than 942 kJ $mole^{-1}$ (the bond energy of N_2), which is necessary for the dissociation of nitrogen molecules.

4. Conclusions

We have demonstrated that cavitation impact initiated by focusing a high-frequency acoustic wave into liquid nitrogen at a frequency ranging from 3 to 6 MHz resulted in semiconductor surface modification up to the microscale pattern formation as well as in a change in the chemical composition of the semiconductor. The morphology of the structures is highly dependent on the exposure parameters and can be controlled by the regulation of acoustic frequency. In particular, a decrease in the characteristic dimension of structures on the semiconductor surface from micrometre to submicrometre size at a frequency changing from 3 to 6 MHz occurs.

Raman spectroscopy data have confirmed the incorporation of nitrogen atoms into GaAs subjected to the acoustic cavitation effect in liquid nitrogen at 3 MHz and the formation of Ga–N bonds and local ordering of N atoms in the alloy lattice. However, the cavitation yield decreases with an increase in frequency in the megahertz range. The question about the possibility of incorporation of nitrogen atoms into the GaAs lattice on increasing the acoustic frequency requires more experiments undoubtedly.

Acknowledgment

The authors are grateful to Dr O Litvin and Dr I Janchuk for their helpful cooperation with the surface characterizations.

References

[1] Ashokkumar M and Mason T 2007 Sonochemistry *Kirk–Othmer Encyclopedia of Chemical Technology* (New York: Wiley)
[2] Kanegsberg B and Kanegsberg E (ed) 2001 Cleaning systems *Handbook for Critical Cleaning* section 2 (Boca Raton, FL: CRC Press)
[3] Bulavin L A and Zabashta Yu F 2007 *Ultrasonic Diagnostics in Medicine* (Leiden: Brill)
[4] Suslick K S, Fang M M, Hyeon T and Mdleleni M M 1999 Applications of sonochemistry to materials synthesis *Sonochemistry and Sonoluminescence* ed L A Crum *et al* (Dordrecht: Kluwer) pp 291–320, and references therein
[5] Gedanken A 2004 *Ultrason. Sonochem.* **11** 47
[6] Wang Y, Tang X, Yin L, Huang W and Gedanken A 2000 *Adv. Mater.* **12** 1183
[7] Landau M V, Vradman L, Herskowitz M, Koltypin Y and Gedanken A 2001 *J. Catal.* **201** 22
[8] Perkas N, Wang Y, Koltypin Yu, Gedanken A and Chandrasekaran S 2001 *Chem. Commun.* 988–989
[9] Flannigan D J and Suslick K S 2005 *Phys. Rev. Lett.* **95** 044301
[10] Bremond N, Arora M, Ohl C D and Lohse D 2006 *Phys. Rev. Lett.* **96** 224501
[11] Brujan E A, Keen G S, Vogel A and Blake J R 2002 *Phys. Fluids* **14** 85
[12] Mettin R 2005 Bubble structures in acoustic cavitation *Bubble and Particle Dynamics in Acoustic Fields: Modern Trends and Applications* ed A A Doinikov (Kerala, India: Research Signpost) pp 1–36
[13] Paufler P, Wagner G and Grosse K 1993 *Cryst. Res. Technol.* **28** 3
[14] SuzukiT, Yasutomi T and Tokuoka T 1999 *Phil. Mag.* A **79** 2637
[15] Domnich V and Gogotsi Yu 2001 High-pressure surface science *Advances in Surface Science* ed H S Nalwa (New York: Academic) pp 355–455
[16] Bournea N K and Field J E 1995 *J. Appl. Phys.* **78** 4423
[17] Arata Y and Zhang Y-C 2002 *Appl. Phys. Lett.* **80** 2416

[18] Prokofyeva T, Sauncy T, Seon M, Holtza M, Qiu Y, Nikishin S A and Temkin H 1998 *Appl. Phys. Lett.* **73** 1409
[19] Mintairov A M, Blagnov P A, Melehin V G, Faleev N N, Merz J L, Qiu Y, Nikishin S A and Temkin H 1997 *Phys. Rev.* B **56** 15836
[20] Page O, Tite T, Bormann D, Tournie E, Maksimov O and Tamargo M C 2003 *Appl. Phys. Lett.* **82** 2808
[21] Jusserand B, Paquet D, Kervarec J and Regreny A 1984 *J. Physique.* **45** C5-145
[22] Wagner J, Maier M, Lauterbach Th, Bachem K H, Fischer A, Ploog K, Morsch G and Kamp M 1992 *Phys. Rev.* B **45** 9120
[23] Katz G and Kosloff R 1995 *J. Chem. Phys.* **103** 9475
[24] Sellers H and Anderson J 2001 *Surf. Sci.* **475** 11